PERGAMON

Phytochemistry 57 (2001) 811–821

PHYTOCHEMISTRY

www.elsevier.com/locate/phytochem

Approaches to understanding the functional architecture of the plant cell wall

Maureen C. McCann[a,*], Max Bush[a], Dimitra Milioni[a], Pierre Sado[a], Nicola J. Stacey[a], Gareth Catchpole[a], Marianne Defernez[b], Nicholas C. Carpita[c], Herman Hofte[d], Peter Ulvskov[e], Reginald H. Wilson[b], Keith Roberts[a]

[a]*Department of Cell Biology, John Innes Centre, Norwich Research Park, Colney, Norwich NR4 7UH, UK*
[b]*Department of Food Metrology, Institute of Food Research, Norwich Research Park, Colney, Norwich NR4 7UA, UK*
[c]*Department of Botany and Plant Pathology, Purdue University, West Lafayette, Indiana 47907-1155, USA*
[d]*Laboratoire de Biologie Cellulaire, INRA, Route de Saint-Cyr, 78026 Versailles cedex, France*
[e]*Biotechnology Group, DIAS, 40 Thornvaldsensvej, DK-1871 Frederiksberg C, Denmark*

Received 16 November 2000; received in revised form 9 March 2001

Abstract

Cell wall polysaccharides are some of the most complex biopolymers known, and yet their functions remain largely mysterious. Advances in imaging methods permit direct visualisation of the molecular architecture of cell walls and the modifications that occur to polymers during growth and development. To address the structural and functional relationships of individual cell wall components, we need to better characterise a broad range of structural and architectural alterations in cell walls, appearing as a consequence of developmental regulation, environmental adaptation or genetic modification. We have developed a rapid method to screen large numbers of plants for a broad range of cell wall phenotypes using Fourier transform infrared microspectroscopy and Principal Component Analysis. We are using model systems to uncover the genes that encode some of the cell-wall-related biosynthetic and hydrolytic enzymes, and structural proteins.

Keywords: *Arabidopsis*; Cruciferae; *Zinnia elegans*; Compositae; Solanum tuberosum; Solanaceae; Fourier transform infrared micro-spectroscopy; cDNA-AFLP; Reflectance confocal scanning laser microscopy; Pectin; Cellulose

1. Introduction

The plant cell wall is a highly organized composite of many different polysaccharides, proteins, and aromatic substances that undergo dynamic changes during cell division, expansion and differentiation (McCann and Roberts, 1991, Carpita and Gibeaut, 1993). However, it has been difficult to ascribe specific functions to these molecules. Molecules of the cell wall must provide mechanical strength, regulate porosity, and control cell-cell adhesion. The functions of the wall are not only mechanical, but also biological. Like the animal extracellular matrix, plant cell walls are a source of signalling molecules that elicit a range of cell behaviours, such as in response to pathogen invasion. Built largely from polysaccharides, the components of the wall are subject to many modifications between the processes of gene expression and assembly in the apoplast. Glycoproteins and polysaccharides are assembled in the Golgi apparatus, enter the secretory pathway in vesicles that release their contents into the apoplast, where cell–wall enzymes act upon their substrates and incorporate them into precise architectures. The current field of cell wall research must encompass the signal transduction mechanisms that result in up- or down-regulation of the

Abbreviations: cDNA-AFLP, complementary DNA-amplified fragment length polymorphism; FTIR, Fourier transform infrared; HGA, homogalacturonic acid; PCA, principal component analysis; PBS, phosphate-buffered saline; RCLSM, reflectance confocal laser scanning microsopy; RG I, rhamnogalacturonan I; TE, tracheary element.

* Corresponding author. Tel.: +44-1603-450687; fax: +44-1603-450022.

E-mail address: maureen.mccann@bbsrc.ac.uk (M.C. McCann).

0031-9422/01/$ - see front matter
PII: S0031-9422(01)00144-3

genes that encode biosynthetic and wall-modifying enzymes, the transcription and translation of those genes, the synthesis of wall polysaccharides by those gene products, and the assembly of the components of the wall into a functional architecture that responds during growth and differentiation to the changing needs of the cell and transmits information back to the protoplast. Such a goal requires both broad and directed views to address the specifics of function. In this paper, we discuss three approaches to characterising cell wall architecture: imaging techniques that probe the location of specific molecules; screening for variation in architecture using IR spectroscopy, and identifying differentially-expressed genes in a model system in which wall synthesis and deposition are the key events.

2. Results and discussion

2.1. Imaging the compositional diversity of walls at the single cell level

The fast-freeze rotary-shadow replica technique has previously been used to directly visualise cell-wall architecture of dicotyledonous species (McCann et al., 1990; Fujino et al., 2000). The images obtained are thought to preserve the native architecture of cell walls, and many thin cross-linking fibres are visible as well as cellulosic microfibrils. In dicots, these cross-linking glycans are xyloglucans — they have a glucan backbone that can hydrogen bond to the surface of cellulose microfibrils and are decorated with xylose-containing side-chains. Xyloglucans are long enough to link two or more microfibrils together to form a network. This network is embedded in a second independent but coextensive network of pectins, the most variable and complex component of the wall. Pectins are loosely defined as polymers rich in galacturonic acid and their associated side-chains, and comprise 20–50% of the wall. Homogalacturonans (HGAs) are long polymers of galacturonic acids that can be methyl-esterified. If methyl groups are removed, then calcium can bind to the carboxylate ions of the galacturonic acid to cross-link them (Goldberg et al., 1996). Some pectins called rhamnogalacturonan I (RGI) are built from a backbone of alternating rhamnose and galacturonic acid residues and carry side-chains of arabinans and galactans.

Dissection of a particular cell type at a specific developmental stage is seldom practical for chemical analysis, which requires microgram to milligram quantities of material. Thus, traditional methods of biochemistry average out the intrinsic heterogeneity of plant tissues (McCann et al., 1997). Two approaches offer the opportunity to analyse wall composition at the single cell level — the use of probes such as antibodies (Knox, 1997), and Fourier transform infrared (FTIR) microspectroscopy (McCann et al., 1997).

Longitudinal and transverse sections of plant stems, roots, or leaves, provide a developmental snapshot of cell growth and differentiation. In the light microscope, the use of probes, such as monoclonal antibodies coupled to fluorescent markers, has revealed the tissue-specific distributions of particular cell components in transverse sections of plant materials (Knox, 1997), whilst longitudinal sections reveal developmental regulation of those components. This is illustrated in Fig. 1 using monoclonal antibodies as designer stains for molecules of the pectin network in potato tubers. Reflectance confocal laser scanning microscopy (RCLSM) allows pectins to be localised to different domains within a wall, even at the light microscope level, by silver enhancement of immuno-gold-labelled tissue and imaging in the confocal microscope (Bush and McCann, 1999). Methyl-esterified pectin is present throughout the walls of parenchymal cells, the galactan side-chains of RGI are next to the plasma membrane but excluded from the middle lamella region that sticks two cells together, and the calcium cross-linked junction zones are localised to the cell corners (Fig. 1a–c). Different tissues contain combinations of different pectic epitopes. Fig. 1d and e shows that parenchymal cells contain both arabinans and galactans, whilst the vascular cells contain arabinans but very little galactan. In the potato stolon, developmental patterns rather than tissue specificity is marked by the presence of arabinan in all of the tissues from the tip to the hook of the stolon, and then calcium pectate and also galactans in all of the tissues beyond the hook (Bush et al., 2001).

Although antibodies are powerful tools, their availability is confined to a small number of wall epitopes and is not comprehensive of the structural complexity of the wall. An alternative technology, called chemical imaging, is becoming available, which combines spatial information with chemical information deduced from relative IR absorbances. In the IR spectrometer, a source emits radiation with a range of frequencies which is then passed through the sample. Particular chemical bonds in the sample absorb radiation of specific frequencies from the beam, and this is plotted as an absorbance spectrum against frequency. IR spectroscopy simultaneously reveals the type, distribution and relative abundances of chemical components within a particular system. However, a single IR spectrum also contains information about the molecular structure and intermolecular interactions among the individual sample components (McCann et al., 1992, 1997). A microscope accessory can be attached such that the infrared beam from the spectrometer is diverted to pass through a sample placed on the microscope stage. The sample can be imaged with visible light and apertures used to restrict the area of sample from which IR spectroscopic data are to be obtained. Therefore, determining the presence and distribution of the chemical constituents within a sample

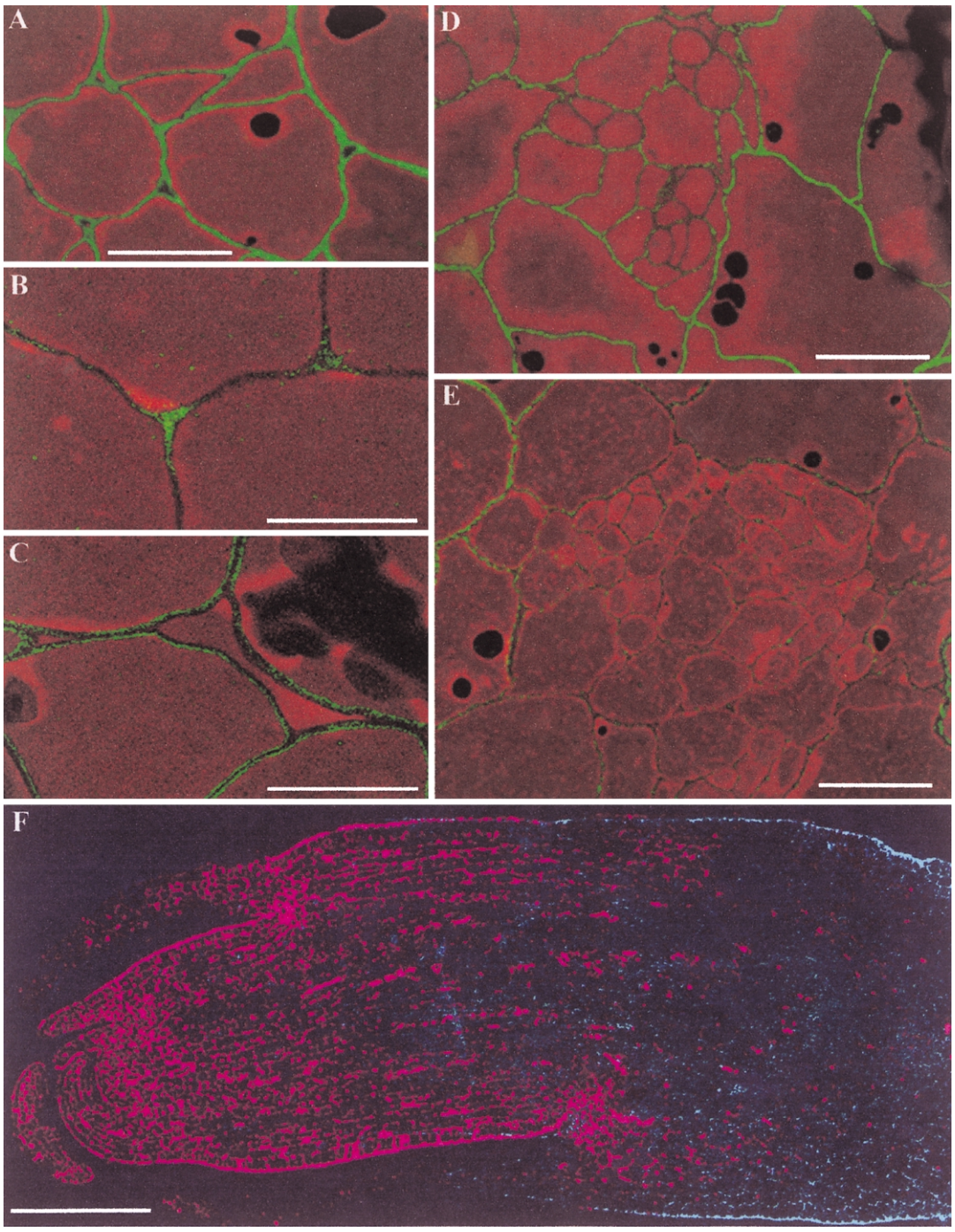

Fig. 1. Potato tuber sections of perimedullary tissue gold-labelled with mAbs (A) JIM 7, (B) 2F4 and (C) LM5 then silver-enhanced and viewed by reflectance confocal microscopy. (A) Methyl-esterified pectic epitopes are throughout the wall, (B) calcium pectate is localised to cell corners, and (C) galactans are present in a region close to the plasma membrane but excluded from the cell corners and middle lamellae. Vascular tissues are labelled with mAb LM6 (D) but label lightly with mAb LM5 (E), indicating the presence of arabinan but very few galactan side-chains of RG1 in these tissues. (F) Longitudinal section of a stolon tip labelled with mAbs 2F4 (blue) and LM6 (pink). The 2F4 epitope is only detected in walls from more proximal regions of the stolon, where it is concentrated in the epidermal and cortical walls. In contrast the LM6 arabinan epitope is localised to walls of young cells at the stolon tip. Scale bars for A, B, C, D, and E represent 20 μm, bar F is 0.5 mm.

depends only on the intrinsic spectral characteristics of the sample, and not on the addition of fluorescent tags or stains. The synergy of what have traditionally been two distinct methods for studying the chemistry and morphology of a sample, IR spectroscopy and optical microscopy, is called chemical imaging.

Current IR microscopes work in two modes. The first mode is single spectrum collection in which data are

collected from a region of the sample as small as 10×10 μm. This is accomplished by limiting the area of a sample illuminated by adjusting an aperture located at a remote image plane. During this process the size of the IR beam focus remains fixed as does the detector area. The maximum size from which a spectrum can be collected is 100×100 μm, which is the size of the detector area. When the smallest usable aperture of 10×10 μm is employed only a fraction of the detector area is illuminated. This small fraction of the detector generates the signal whilst the entire detector area generates noise. Consequently the spectroscopic performance falls dramatically with the size of aperture used.

The second mode of operation is mapping (McCann et al., 1997). In this mode the sample is moved under computer control such that different areas of the sample are measured in turn. Eventually an array of spectra is generated. These spectra can be correlated with visual images of the sample so that optically observed features can be associated with functional groups. While contrast in MRI images is determined by differences in the NMR spectrum of the sample components, contrast in IR spectroscopic imaging is determined by differences in the vibrational spectral response. It is possible to generate a contour plot (map) of the distribution of functional groups within a sample, using colour to represent absorbance intensities.

A 3-day-old maize coleoptile was sectioned transversely by hand, cleared of its soluble material and mounted on a barium fluoride window for chemical imaging. Mapping software allowed the collection of 273 individual FTIR spectra with an aperture size of 25×25 μm in an array encompassing epidermal, vascular and mesophyll cells from a transverse section of one-quarter of the coleoptile (Fig. 2a). The spectra in the data set were first area-normalised to compensate for any changes in thickness across the section. Peaks corresponding to phenolic esters (1720 cm^{-1}) or to methyl esters (1740 cm^{-1}) were enriched in the vascular bundle, and slightly enhanced in the outer epidermis (Fig. 2b, c). A peak corresponding to phenolic ring absorbance (1515 cm^{-1}) is enriched in the vascular tissue, and is decreased in the inner epidermis (Fig. 2d). The chemical images thus indicate some differences between the inner and outer epidermis. Absorbances at 1000 and 1020 cm^{-1} are enriched in the mesophyll layer (Fig. 2e, f), whilst absorbances at 1090 and 1034 cm^{-1} are enriched in the epidermal tissues (Fig. 2g, h). These latter two absorbances are potentially diagnostic for the presence of glucomannans (Kacuràková et al., 2000). These data demonstrate the ability of chemical imaging to localise different chemical species to specific cell types and the large heterogeneities in wall composition within the maize coleoptile. A new generation of instruments are becoming available that combine an IR microscope with focal plane array detector. These devices collect spectra simultaneously from all points in a field of view, reducing collection times for equivalent samples from a few hours to a few minutes.

2.2. Detecting cell walls of altered composition

Why cell walls are structurally complex seems obvious — cell walls must function in cell–cell adhesion, signal transduction both cell-to-cell and environment-to-cell, cell division, growth and differentiation, but how the molecular machinery of the wall is assembled and later modified to carry out those functions is still unknown. By studying cell walls with altered compositions, either as a consequence of developmental regulation, environmental adaptation, or genetic modification, we can assess the effect of such modifications on cell wall properties and on plant development. The selection of mutant plants with altered cell wall compositions and architectures is particularly useful because of the wide range of potential modifications and the possibility of uncovering novel genes that encode enzymes that participate in biosynthetic pathways, wall assembly, or in modifications to polymers in muro (Reiter, 1998). Mutants with altered cellulose deposition have been identified directly by birefringence (Potikha and Delmer, 1995). Other cell-wall mutations have appeared serendipitously in the course of screens for developmental phenotypes, such as a temperature-sensitive radial cell swelling mutant that was cellulose-deficient (Baskin et al., 1992, Arioli et al., 1998) or a collapsed xylem phenotype (Turner and Somerville, 1997).

Mutations in non-cellulosic polysaccharides may not always have visually abnormal or otherwise predictable phenotypes, and, hence, a general method is necessary to select for a broad range of potential modifications. One method that has been successfully applied is to screen directly for neutral sugars of cell-wall polymers that are over- or under-represented when compared with their distribution in the walls of a wild-type population (Reiter et al., 1997). This screen employs derivatisation of the cell-wall non-cellulosic sugars from leaves to alditol acetates, with subsequent quantitation by gas–liquid chromatography. Sugar composition can be assayed with great precision by this method, but the large numbers of plants involved in a mutant screen make it labour-intensive. FTIR microspectroscopy is an extremely rapid, non-invasive vibrational spectroscopic method that can quantitatively detect a range of functional groups including carboxylic esters, phenolic esters, protein amides and carboxylic acids, and can provide a complex "fingerprint" of carbohydrate constituents and their organization (McCann et al., 1992, 1997; Séné et al., 1994). The time taken to acquire a spectrum of a sample is roughly 30 s. It is non-destructive and does not require derivatization of the sample, so further assays can be applied to the same sample once potential mutants are identified.

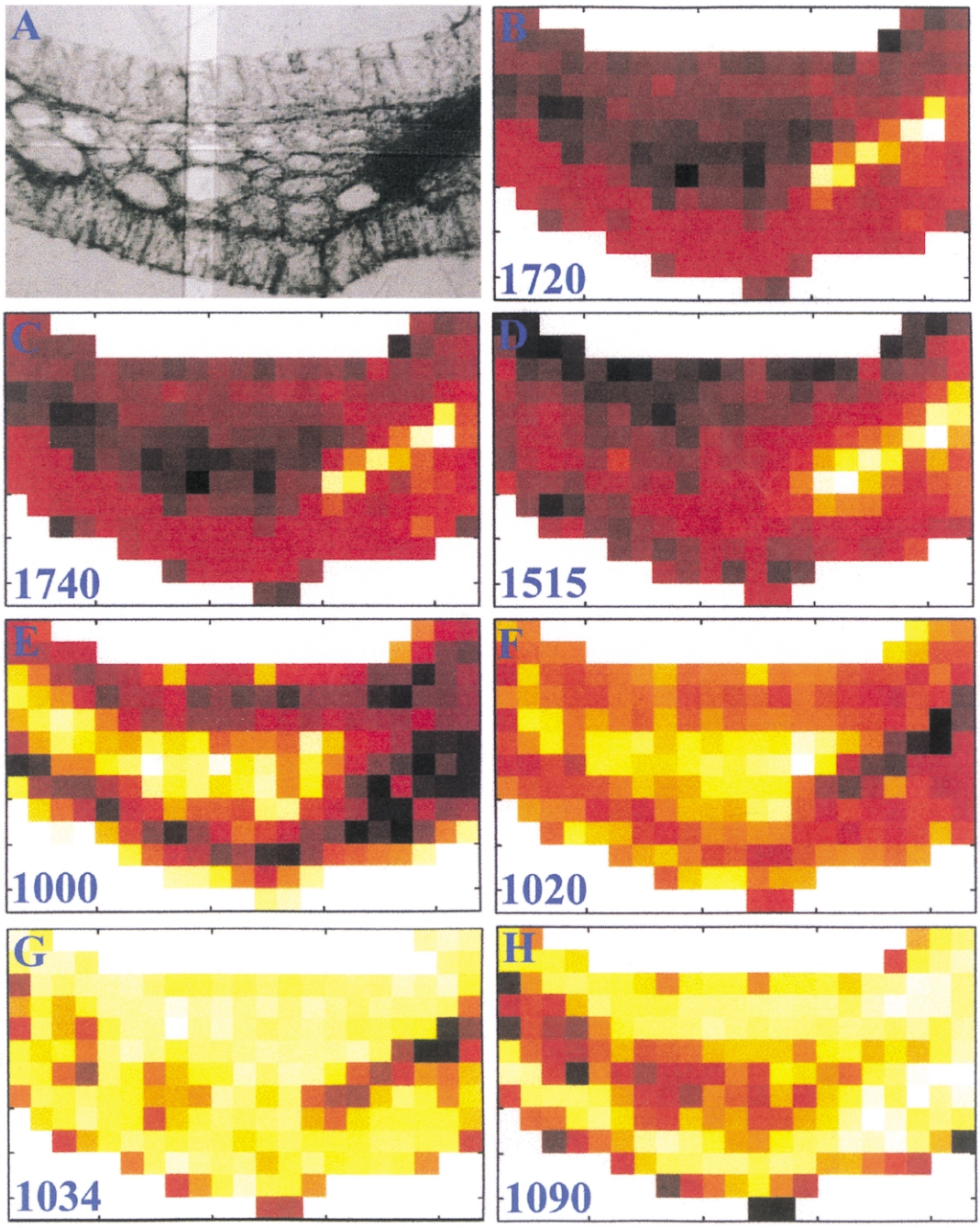

Fig. 2. Chemical images of a transverse section of 3-day-old maize coleoptile derived from FTIR spectra sampled with a 25×25 μm window. (A) Brightfield micrograph of the coleoptile section using mirror optics in the IR microscope. An example of the area from which IR data is sampled is delimited by a pair of transparent double-bladed apertures. (B) Phenolic esters of uronic acids sampled at 1720 cm^{-1}. (C) Carboxyl esters sampled at 1740 cm^{-1}. (D) Aromatic substances sampled at 1515 cm^{-1}. (E) Absorbance intensity at 1000 cm^{-1}. (F) Absorbance intensity at 1020 cm^{-1}. (G, H) Absorbances at 1034 and 1090 cm^{-1}, respectively, characteristic of glucomannan.

The effective analysis of large data sets of spectra is complex and the use of multivariate data reduction techniques (Massart et al., 1988) is now standard practice for many applications. Spectra are not analog, but are constructed from data points collected at intervals of 8 cm^{-1}. Principal component analysis (PCA) is a widely-used mathematical technique that is used to reduce the dimensionality of the data from the several hundred data points in the original spectra to a fewer number of dimensions (Kemsley, 1998). The variability in each individual spectrum relative to the mean of the population can then be represented as a smaller set of values (axes) termed principal components (see Fig. 3). The effect of this process is to concentrate the sources of

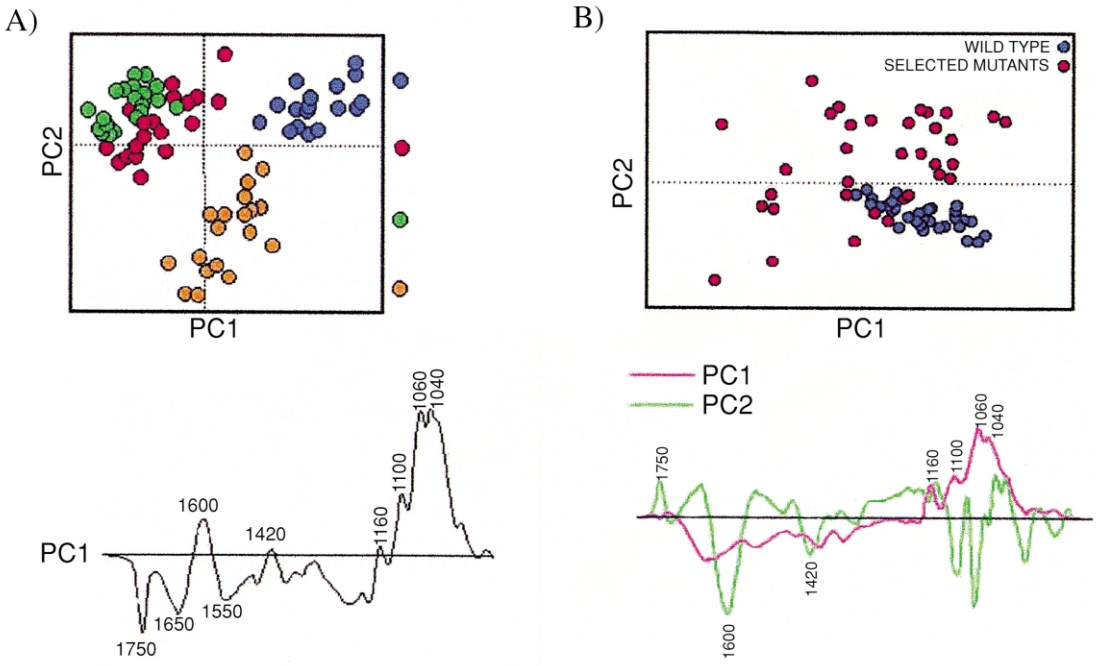

Fig. 3. Exploratory PCA of IR spectra sampled from populations of *Arabidopsis* hypocotyls. (A) Relative cellulose content of populations can be estimated from their scores on PC1, a loading with characteristic features of cellulose (Liang and Marchessault, 1959). Peaks associated with pectin are negatively correlated in the loading. The *rsw1* mutants discriminate on PC2 probably because they are in a different ecotype background. (B) Some dwarf hypocotyl mutants can be discriminated from wild-type on the basis of two principal components, PC1 has features of cellulose (Liang and Marchessault, 1959) whilst PC2 shows features of pectin (Sene et al., 1994).

variability in the data into the first few PCs. Plots of the so-called PC scores (projection on to PC axes) against one another can reveal clustering or structure in the data set.

We established and validated a model that can discriminate between the leaves of wild-type and a previously defined set of cell-wall mutants of *Arabidopsis*. Exploratory PCA indicated that mutants deficient in different cell-wall sugars are distinguished from each other (Chen et al., 1998). We have also used IR microspectroscopy to screen a population of hypocotyl mutants for alterations in their cell walls. The *Arabidopsis* hypocotyl mutants were selected from seedlings that are dwarf when dark-grown, and thus affected in cell elongation (Gendreau et al., 1997). The hypocotyl is laid down by a set of programmed cell divisions during early embryogenesis. Post-embryogenic growth of this organ involves no further cell divisions and so separates the events of cell division from those of cell expansion.

From a pre-selected sample of 40 dwarf mutants, PCA shows that both pectic (Sene et al., 1994) and cellulosic (Liang and Marchessault, 1959) features in the FTIR spectra can be used to discriminate mutants from a population of wild-type (Fig. 3). The wild-type population shows that a tight ratio exists under normal growth conditions, but this proportionality is disrupted in the mutants. PCA also revealed a dose-dependent reduction in cellulose content within hypocotyls treated with increasing concentrations of dichlorobenzonitrile (DCB), an inhibitor of cellulose synthesis. Cellulose deficiency was also detected in hypocotyl cell walls of *rsw1*, a temperature-sensitive mutant when grown at the restrictive temperature for a gene encoding the catalytic subunit of cellulose synthase (Arioli et al., 1998). The *kor* mutation (*korrigan*) is a mutation in a gene encoding an endo-glucanase (Nicol et al., 1998). Analysis of FTIR spectra of *rsw1*, *kor*, and DCB-treated seedlings showed that cellulose deficiency was invariably associated with an increased pectin content (Fig. 3). These observations are consistent with earlier results using suspension-cultured cells of tomato adapted to growth on DCB which make a pectin-rich wall that virtually lacks a cellulose-xyloglucan network (Shedletzky et al., 1990). The formation of one network has been prevented, while the other is still able to provide a cell wall with at least some of its usual functions.

Transgenic materials in which cell-wall-related genes have been up- or down-regulated provide a useful complement to mutants. We are also studying transgenic potato tubers in which fungal cell-wall enzymes have been over-expressed in a tuber-specific manner as a means to valorise the waste from starch production (Vincken et al., 2000). Removal of galactans by apoplastic expression of a fungal galactanase resulted in normal tuber development (Oxenbøll-Sørensen et al., 2000). We used PCA of IR spectra to screen a number

of transgenic lines, and selected one line that can be distinguished from the relevant control because of changes in pectic characteristics (Fig. 4a). Immuno-gold labelling confirmed that this line indeed had a greatly reduced galactan content (Fig. 4b–e).

2.3. Expression profiling — a molecular approach to identify genes that encode cell-wall related proteins

The wall contains structural proteins as well as hundreds of different cell-wall enzymes, and polysaccharides are the

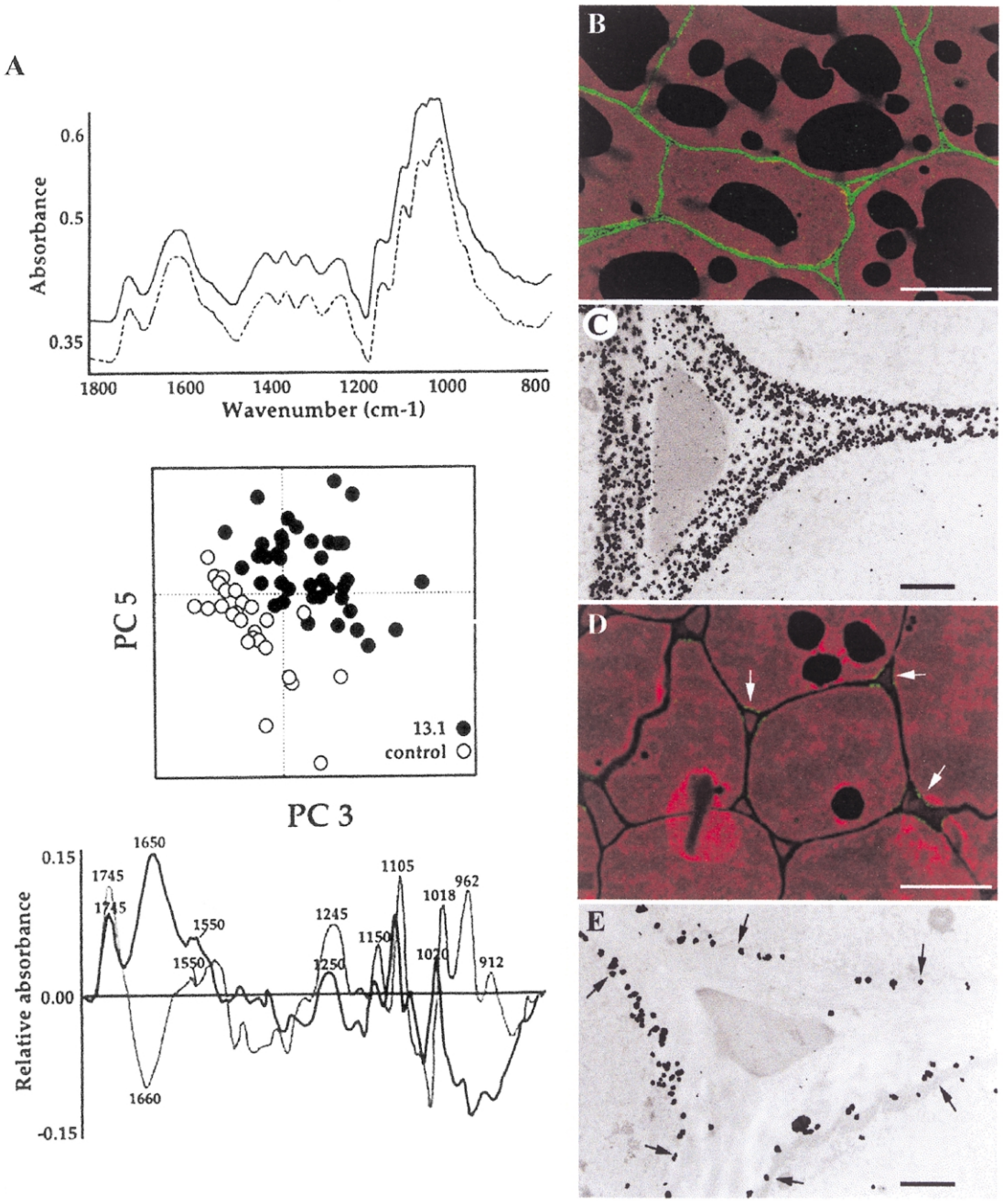

Fig. 4. (A) Top: averaged FTIR spectra of potato tuber cortex from 20 wild-type tubers (solid line) and 20 transgenic tubers (dashed line) over-expressing a fungal galactanase targetted to the apoplast. Middle. Exploratory PCA discriminates the transgenic population from the wild type, using the third and fifth PC scores. The loadings for PC3 (black line) and PC5 (gray line) show features characteristic of pectins at 1745, 1250, 1150, 1105 and 1018 cm^{-1}. Sections of wild-type tuber gold-labeled with mAb LM5, that recognises a galactan epitope, and imaged by RCLSM (B) and in the TEM (C), and equivalent of the galactanase transformant (D, E). The walls of wild-type parenchymal cells are strongly labelled (green in A, black particles in B) whereas in the transformant, the labelling density is greatly reduced and localised only to some cell corners (arrows) close to the plasma membrane. Scale bars represent 100 μm for RCLSM images and 2 μm for electron micrographs.

products of biosynthetic enzymes. The genes that encode these classes of cell-wall-related proteins belong to large multi-gene families. Much work remains to be done to elucidate the functions of the different family members, and to identify cell-wall-related genes without sequence identities. We are using a model system in which synthesis and deposition of cell wall is the main event, to identify cell-wall-related genes involved specifically in xylogenesis.

The construction of a tracheid or xylem element involves deposition of thick reinforcing hoops of secondary cell wall, waterproofing it with lignin followed by autolysis of the cell contents. In a plant, only a few cells are in the process of forming xylem, but we can study this entire developmental pathway in vitro using the *Zinnia* mesophyll cell system originally developed by Fukuda and Komamine (1980). In our laboratory, the *Zinnia* system consists of mesophyll and palisade cells isolated from the leaves of *Zinnia elegans* cv. Envy that are put into liquid culture and supplied with two plant growth factors, auxin and cytokinin, after 48 h (McCann et al., 2000). In a further 48 h, over half of the living cells have synchronously undergone trans-differentiation, making it possible to precisely stage the events involved in building a TE. Thus, one cell type can be reproducibly and synchronously switched, with known external signals, into a different cell type.

We have recently applied a novel RNA finger-printing technology, cDNA-AFLP (Bachem et al., 1996, Durrant et al., 2000), that allowed the detection of differentially-regulated genes across the time-course of xylo genesis. cDNAs are synthesized from mRNA populations isolated from the *Zinnia* cultures at five time-points, digested with a pair of restriction enzymes, adaptor-ligated and amplified by PCR to produce the primary template. A subset of this population of fragments is selectively amplified using primers with two selective nucleotides, and then analysed on polyacrylamide gels. Over 600 genes, whose transcription show overt changes in abundance over time, have been selected and partial sequences obtained. These sequences were then compared with databases from the plant and animal genome sequencing projects, allowing an identity to be assigned to about half of the predicted gene products, including about 10% that encode cell wall biosynthetic enzymes, hydrolytic enzymes or structural proteins (manuscript in preparation).

The deposition of hoops of secondary wall material occurs at 90–96 h of culture (between 42 and 48 h after

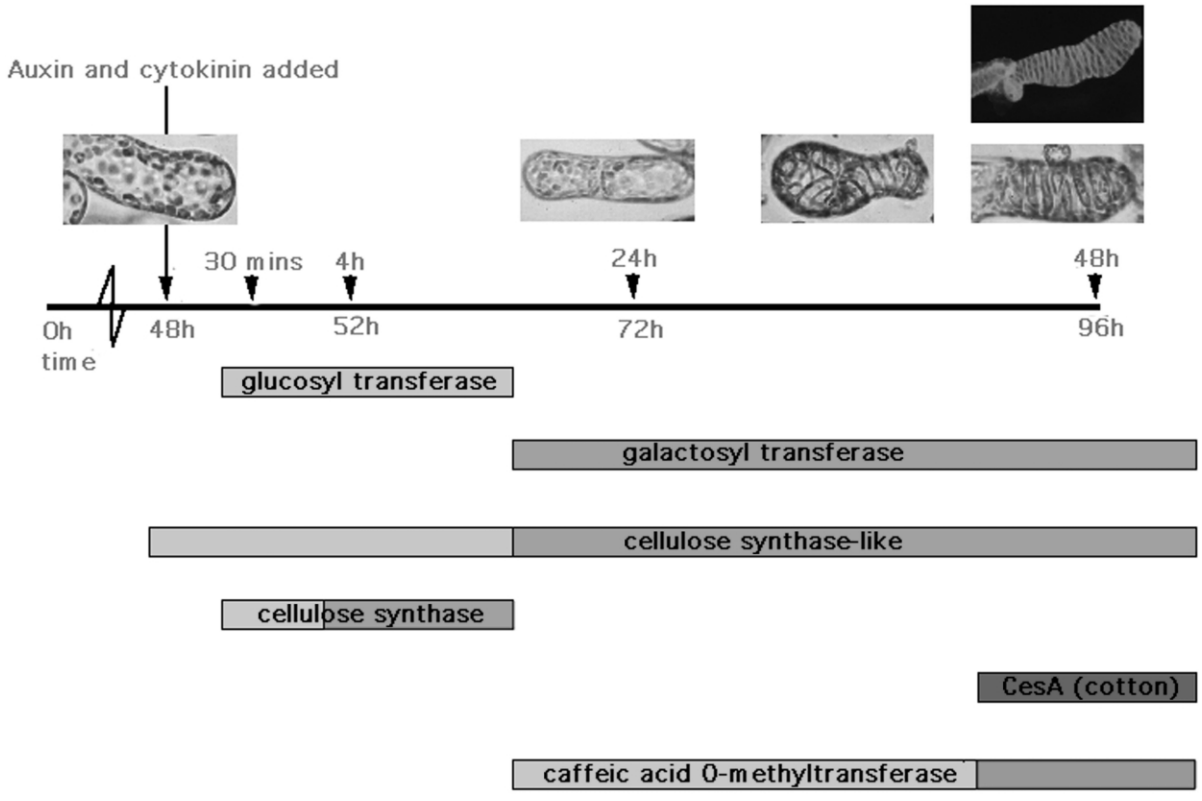

Fig. 5. Time course of the trans-differentiation of isolated *Zinnia* mesophyll cells to tracheary elements and the expression patterns of six cell wall biosynthetic genes identified so far by the cDNA-AFLP screen. Micrographs, left to right. (1) A palisade parenchyma cell appears unchanged after 48 h in liquid culture without TE-inducing growth factors. Auxin and cytokinin are added at 48 h, and RNA is extracted at this time and then 30 min, 4 h, 24 h and 48 h later. (2) At the 16 h point after induction, the chloroplasts move to the cell edges, and most of the cells have divided. (3) By 42 h after induction, the secondary wall thickenings have been deposited. (4) By 48 h after induction, the thickenings become lignified, and can be stained with phloroglucinol (above). Shading intensities of the bars indicate relative abundance of the cDNA-AFLP fragment in the gel.

addition of auxin and cytokinin). We have over 50 partial sequences of cell-wall related genes, many of which are hydrolytic enzymes (Milioni et al., 2001). Fig. 5 shows the expression patterns of six of the sequences that encode biosynthetic enzymes. A cellulose synthase is up-regulated early, perhaps simply induced by auxin, and a late-expressed cellulose synthase has high sequence identities with an Arabidopsis sequence (AB006703), the cotton cellulose synthase that is expressed in differentiating cotton fibers (Holland et al., 2000), and with a xylem-specific cellulose synthase gene from aspen (Wu et al., 2000). There are two sugar transferases for adding sugars to non-cellulosic polymers and a cellulose-synthase-like gene, which may encode a biosynthetic enzyme making a different polymer backbone. The enzyme caffeic acid *O*-methyltransferase from the lignin biosynthetic pathway is also expressed. About 40% of our sequences are unknowns — either hypothetical proteins in the *Arabidopsis* database or not represented in any of the plant or animal databases. As known genes encoding cell wall-related proteins comprise about 10% of our 600 sequences, then there may be further 30 sequences that represent cell-wall-related proteins of totally unknown function.

3. Conclusion

Genetically-defined variation through mutant approaches or transgenic technologies offers the best opportunity to identify a broad range of structural and architectural alterations in cell walls, leading to improved understanding of plant cell growth and differentiation. Gene discovery in the *Zinnia* system will have relevance for many commercially important tree species. By defining the key structural components in *Arabidopsis*, there is the opportunity to define wall properties in which variation is economically desirable include the length, substitution, and cross-linking of pectic polysaccharides, the relative levels of cellulose, the length and mechanical properties of fibres, the relative allocation of carbon to wall biomass, the regulation of cell–cell adhesion, wall-based growth control, and lignin composition, architecture, distribution and amount.

4. Experimental

4.1. Tissue preparation for immunocytochemistry

Elongating stolons and mature tubers were cut from mature *Solanum tuberosum* (L.) plants (cv. Karnico) and immersed in 2.5% (v/v) glutaraldehyde (EM grade) in 0.05 M sodium cacodylate containing 0.05% (v/v) NP-40 (Sigma, Poole, UK). All of the samples were processed for low temperature L.R. White resin embedding as described previously (Bush and McCann, 1999).

4.2. Immunogold labelling

Blocks of tissue were sectioned: 0.5-μm thick resin sections were collected on multi-well glass slides for light microscopy and ultrathin sections for electron microscopy were collected on Formvar-carbon coated gold grids. The sections were labelled as described previously (Bush and McCann, 1999), with mAbs that recognise the following pectic epitopes; JIM 7, $\geqslant$35% methyl-esterified homogalacturonan (Knox et al., 1990); 2F4, a calcium-dependent conformational epitope of at least nine contiguous galacturonic acid residues (Liners et al., 1989); LM5, (1→4)-β-D-galactan (Jones et al., 1997); LM6, (1→5)-α-L-arabinan (Willats et al., 1998). After three 10 min washes in phosphate-buffered saline (PBS) the sections were incubated with 5 nm gold conjugates (British BioCell International) overnight at 4°C. Sections were washed in PBS again, fixed in 1% (v/v) glutaraldehyde, and finally rinsed thoroughly with distilled water prior to silver enhancement. Control sections were treated in parallel but with the omission of the primary mAb. Silver enhancement of 5 nm gold probes was performed for 2 min at 20°C for electron microscopy, but this was extended to 10–15 min for light microscopy; the BioCell silver enhancement kit (British BioCell International) was used according to the manufacturer's instructions.

4.3. Reflectance confocal laser scanning microsopy (RCLSM)

Gold-labelled and silver-enhanced 0.5 μm-thick resin sections were counter-stained with basic fuchsin and examined with a Leica TCS NT laser scanning confocal microscope, using an RT 30/70 mirror and excitation and emission wavelengths of 488 and $>$515 nm, respectively. Images of autofluorescence and epi-reflectance were recorded separately, and merged and processed with Adobe Photoshop 4.0. Ultrathin sections counter-stained with uranyl acetate and lead citrate were examined in a Jeol 1200EX transmission electron microscope.

4.4. FTIR microspectroscopy and chemical imaging

The Arabidopsis hypocotyls were placed on 2-mm thick×13-mm diameter barium fluoride windows, and the materials were air-dried at 37°C for about 1 h. The windows were supported on the stage of a UMA500 microscope accessory of a Bio-Rad FTS175c FTIR spectrometer equipped with a liquid nitrogen-cooled mercury cadmium telluride detector. An area of wall (100×100 μm) was selected for spectral collection in

transmission mode. One hundred and twenty-eight interferograms were collected with 8 cm^{-1} resolution and co-added to improve the signal-to-noise ratio for each sample. Three spectra were collected from different areas of each hypocotyl, avoiding the stele and then averaged and baseline-corrected.

For chemical imaging, transverse sections were hand-cut from 3-day-old maize coleoptiles that were frozen in a cryosectioning medium (Tissue-Tek, Agar UK). Sections about 50 μm thick were picked up onto barium fluoride windows. The sections adhering to the surface were then washed extensively with water to remove all traces of the sectioning medium. A small amount of the sectioning medium was also streaked across a barium fluoride window as a control. FTIR spectra were acquired with an aperture size of 25×25 μm from an array encompassing epidermal, vascular and mesophyll cells from transverse sections comprising about 25% of the coleoptile area.

4.5. Preparation of cell cultures

Seeds of *Zinnia elegans* c. Envy (Chiltern Seeds Ltd, UK) were germinated in a peat/sand potting compost in a controlled environment room at 20°C with a 16 h day. The first true leaves of 14-day-old plants were removed, surface-sterilised in 5% commercial NaOCl, and rinsed three times in sterile distilled water. Single cells were isolated by gently grinding the leaves in 0.2 M mannitol in a mortar and pestle. The suspension was filtered through two layers of muslin and washed three times in 0.2 M mannitol by spinning at 800 rpm for 2 min. Cells were resuspended in culture medium (Fukuda and Komamine, 1980) with no hormones (maintenance medium), or 1 mg l^{-1} BAP and 1 mg l^{-1} NAA (inductive medium). Cultures were maintained at 27°C in the dark, shaking at 80 rpm, with 3 ml of cell suspension per well in six-well plates (Sterilin, UK) at a density of 10^6 cells ml^{-1}. At 48 h, cells were transferred by pipetting media and cells from the wells in the six-well plates into 30-ml screw-cap tubes (Sterilin, UK), spinning the tubes at 800 rpm for 2 min, pouring off the supernatant and re-suspending the cells in new medium at the same cell density of 10^6 cells ml^{-1}.

4.6. cDNA-AFLP

Total RNA was extracted from *Zinnia* cells at different stages of in vitro TE formation, according to Shirzadegan et al. (1991). Poly(A^+) RNA was obtained by using magnetic oligo(dT)25 Dynabeads, according to the manufacturer's (DYNAL, UK) instructions. Synthesis of the first strand of cDNA was carried out with Expand Reverse Transcriptase (Boehringer Mannheim), as described by the manufacturer. The second strand cDNA synthesis was performed according to Gubler et al. (1983). cDNA-AFLP was performed according to Bachem et al. (1996) and Durrant et al. (2000). The AFLP products were analyzed on a 6% polyacrylamide denaturing gel, at constant power (90 W) until the bromophenol blue dye reached the bottom. Gels were dried under vacuum at 80°C and exposed to X-ray films (KODAK X-OMAT AR) for autoradiography.

4.7. Isolation of cDNA clones and sequence data analysis

The cDNA bands of interest were marked and the X-ray films were repositioned on the radioactive gels. The segments of interest were cut out with a surgical blade, eluted and re-amplified with the same primer set as used for the initial amplification. The re-amplified cDNAs were subcloned using the pGEM-T easy vector system (PROMEGA). For each re-amplified fragment, several independent *E. coli* colonies were selected and the inserted fragments were sequenced on an automated sequencer using the BigDye Terminator kit (Applied Biosystems). Each sequence was analyzed against the sequences in Genbank non-redundant and expressed sequence tag (EST) databases using the BlastN programme for nucleic acids and the BlastX programme for proteins at the NCBI web server (Altschul et al., 1997). Default parameters of the programmes were used in both cases.

Acknowledgements

We are grateful to Drs. J.P. Knox and P. Van Cutsem for their kind gifts of mAbs. We would like to thank Kate Kemsley for advice on using PCA and LDA, Grant Calder for assistance with the Leica confocal microscope, Sue Bunnewell for photographic assistance, and Dr. Jonathon Jones and Dr. Wendy Durrant for assistance and advice with the cDNA-AFLP screen. NJS, MD, GC, RHW and KR gratefully acknowledge the financial support of the BBSRC. DM is funded by an EU Marie Curie Fellowship, MB is funded by an EU network grant, PS is funded by a BBSRC special studentship, NCC is funded by a grant from the US National Science Foundation Genome Research Program, and MCM is funded by a Royal Society University Research Fellowship.

References

Altschul, S.F., Madden, T.L., Schaffer, A.A., Zhang, J.H., Zhang, Z., Miller, W., Lipman, D.J., 1997. Gapped BLAST and PSI-BLAST: a new generation of protein database search programs. Nucl. Acid Res. 25, 3389–3402.

Arioli, T., Peng, L.C., Betzner, A.S., Burn, J., Wittke, W., Herth, W., Camilleri, C., Hofte, H., Plazinski, J., Birch, R., Cork, A., Glover,

J., Redmond, J., Williamson, R.E., 1998. Molecular analysis of cellulose biosynthesis in *Arabidopsis*. Science 279, 717–720.

Bachem, C.W.B., vanderHoeven, R.S., deBruijn, S.M., Vreugdenhil, D., Zabeau, M., Visser, R.G.F., 1996. Visualization of differential gene expression using a novel method of RNA fingerprinting based on AFLP: Analysis of gene expression during potato tuber development. Plant J. 9, 745–753.

Baskin, T.I., Betzner, A.S., Hoggart, R., Cork, A., Williamson, R.E., 1992. Root morphology mutants in *Arabidopsis thaliana*. Aust. J. Plant Physiol. 19, 427–437.

Bush, M.S., McCann, M.C., 1999. Pectic epitopes are differentially expressed in the cell walls of potato (*Solanum tuberosum*) tubers. Physiol. Plant. 107, 201–213.

Bush, M., Marry, M., Huxham, I.M., Jarvis, M.C., McCann, M.C., 2001. Developmental regulation of pectic epitopes during potato tuberisation Planta, in press.

Carpita, N.C., Gibeaut, D.M., 1993. Structural models of primary cell walls in flowering plants: consistency of molecular structure with the physical properties of the walls during growth. Plant J. 3, 1–30.

Chen, L., Carpita, N.C., Reiter, W-D., Wilson, R.H., Jeffries, C., McCann, M.C., 1998. A rapid method to screen for cell-wall mutants using discriminant analysis of Fourier transform infrared spectra. Plant J. 16, 385–392.

Durrant, W.E., Rowland, O., Piedras, P., Hammond-Kosack, K.E., Jones, J.D.G., 2000. cDNA-AFLP reveals a striking overlap in race-specific resistance and wound response gene expression profiles. Plant Cell 12, 163.

Fujino, T., Sone, Y., Mitsuishi, Y., Itoh, T., 2000. Characterization of cross-links between cellulose microfibrils, and their occurrence during elongation growth in pea epicotyl. Plant Cell Physiol 41, 486–494.

Fukuda, H., Komamine, A., 1980. Establishment of an experimental system for the tracheary element differentiation from single cells isolated from the mesophyll of *Zinnia elegans*. Plant Physiol. 52, 57–60.

Gendreau, E., Traas, J., Desnos, T., Grandjean, O., Caboche, M., Hofte, H., 1997. Cellular basis of hypocotyl growth in *Arabidopsis thaliana*. Plant Physiol. 114, 295–305.

Goldberg, R., Morvan, C., Jauneau, A., Jarvis, M.C., 1996. Methyl-esterification, de-esterification and gelation of pectins in the primary cell wall. In: Visser, J., Voragen, A.G.J. (Eds.), Pectins and Pectinases. Elsevier Science, Amsterdam, pp. 166–189.

Gubler, U., Monahan, J.J., Lomedico, P.T., Bhatt, R.S., Collier, K.J., Hoffman, B.J., Bohlen, P., Esch, F., Ling, N., 1983. Cloning and sequence analysis of cDNA for the precursor of human growth hormone-releasing factor, somatocirinin. Proct. Nat. Acad. Sci. 80, 4311–4314.

Holland, N., Holland, D., Helentjaris, T., Dhugga, K., Xoconostle-Cazares, B., Delmer, D.P., 2000. A comparative analysis of the plant cellulose synthase (CesA) gene family. Plant Physiol. 123, 1313.

Jones, L., Seymour, G.B., Knox, J.P., 1997. Localization of pectic galactan in tomato cell walls using a monoclonal antibody specific to (1→4)-β-D-galactan. Plant Physiol. 113, 1405–1412.

Kacuráková, M., Capek, P., Sasinková, V., Wellner, N., Ebringerová, A., 2000. FT-IR study of plant cell wall model compounds: pectic polysaccharides and hemicelluloses. Carbohydr. Polymers 43, 195–203.

Kemsley, E.K., 1998. Discriminant Analysis of Spectroscopic Data. John Wiley and Sons, Chichester, UK.

Knox, J.P., Linstead, P.J., King, J., Cooper, C., Roberts, K., 1990. Pectin esterification is spatially regulated both within cell walls and between developing tissues of root apices. Planta 181, 512–521.

Knox, J.P., 1997. The use of antibodies to study the architecture and developmental regulation of plant cell walls. Int. Rev. Cytol. 171, 79–120.

Liang, C.Y., Marchessault, R.H., 1959. Infrared Spectra of Crystalline Polysaccharides. II. Native Celluloses in the region from 640 to 1700 cm^{-1}. J. Polymer Science XXXIX, 269–278.

Liners, F., Letesson, J-J., Didembourg, C., Van Cutsem, P., 1989. Monoclonal antibodies against pectin, Recognition of a conformation induced by calcium. Plant Physiol. 91, 1419–1424.

Massart, D.L., Vandeginste, B.G.M., Deming, S.N., Michotte Y., Kaufman, L. 1988. In Vandeginste B.G.M., Kaufman, L. Data handling in Science and Technology. Vol. 2: Chemometrics, a Textbook. Elsevier Science, Amsterdam.

McCann, M.C., Wells, B., Roberts, K., 1990. Direct visualisation of cross-links in the primary plant cell wall. J. Cell Sci. 96, 323–334.

McCann, M.C., Roberts, K., 1991. Architecture of the primary cell wall. In: Lloyd, C.W. (Ed.), The Cytoskeletal Basis of Plant Growth and Form. Academic Press, London, pp. 109–129.

McCann, M.C., Hammouri, M.K., Wilson, R.H., Belton, P.S., Roberts, K., 1992. Fourier transform infrared microspectroscopy is a new way to look at plant cell walls. Plant Physiol. 100, 1940–1947.

McCann, M.C., Chen, L., Roberts, K., Kemsley, E.K., Séné, C., Carpita, N.C., Stacey, N.J., Wilson, R.H., 1997. Infrared microspectroscopy: sampling heterogeneity in plant cell wall composition and architecture. Physiol. Plant 100, 729–738.

McCann, M.C., Domingo, C., Stacey, N.J., Milioni, D., Roberts, K., 2000. Chapter 37: Tracheary element formation in an in vitro system. In: Savidge, R., Barnett, J., Napier, R. (Eds.), Cambium: the Biology of Wood Formation. BIOS Scientific Publishers LTD, Oxford, pp. 457–470.

Milioni, D., Sado, P-E., Stacey N.J., Roberts, K., McCann M.C. 2001. Differential expression of cell-wall-related genes during formation of tracheary elements in the *Zinnia* mesophyll cell system. Plant Molecular Biology.

Nicol, F., His, I., Jauneau, A., Vernhettes, S., Canut, H., Höfte, H., 1988. A plasma membrane-bound putative endo-1,4-β-D-glucanase is required for normal wall assembly and cell elongation in *Arabidopsis*. EMBO J. 17, 5563–5576.

Oxenbøll-Sørensen, S., Pauly, M., Bush, M., Skjøt, M., McCann, M.C., Borkhardt, B., Ulvskov, P., 2000. Pectin engineering: Modification of potato pectin by in vivo expression of an endo-1,4-β-D-galactanase. Proc. Natl. Acad. Sci. USA 97, 7639–7644.

Potikha, T., Delmer, D.P., 1995. A mutant *Arabidopsis thaliana* displaying altered patterns of cellulose deposition. Plant J. 7, 453–460.

Reiter, W-D., Chapple, C.C.S., Somerville, C.R., 1999. Mutants of *Arabisopsis thaliana* with altered cell wall polysaccharide composition. Plant J. 12, 335–345.

Reiter, W-D., 1998. *Arabidopsis thaliana* as a model system to study synthesis, structure, and function of the plant cell wall. Plant Physiol. Biochem. 36, 167.

Séné, C.F.B., McCann, M.C., Wilson, R.H., Grinter, R., 1994. FT-Raman and FT-infrared spectroscopy: an investigation of five higher plant cell walls and their components. Plant Physiol. 106, 1623–1633.

Shedletzky, E., Shmuel, M., Trainin, T., Kalman, S., Delmer, D.P., 1990. Adaptation and growth of tomato cells on the herbicide 2,6-dichlorobenzonitrile (DCB) leads to production of unique cell walls virtually lacking a cellulose-xyloglucan network. Plant Phys 94, 980–987.

Shirzadegan, M., Christie, P., Seemann, J.R., 1991. An efficient method for isolation of RNA from tissue cultured plant cells. Nucl. Acid Res. 19, 6055.

Turner, S.R., Somerville, C.R., 1997. Collapsed xylem phenotype of *Arabidopsis* identifies mutants deficient in cellulose deposition in the secondary cell wall. Plant Cell 9, 689–701.

Vincken, J.P., Borkhardt, B., Bush, M., Doeswijk-Voragen, C., Dopico, B., Labrador, E., Lange, L., McCann, M., Morvan, C., Muñoz, F., Oomen, R., Peugnet, I., Rudolph, B., Schols, H., Sørensen, S., Ulvskov, P., Voragen, A., Visser, R., 2000. Remodelling pectin structure in potato. In: de Vries, G.E., Metzlaff, K. (Eds.), Conference Proceedings of Phytosfere '99 European Plant Biotechnology Network. Elsevier Science, pp. 23–34.

Willats, W.G.T., Marcus, S.E., Knox, J.P., 1998. Generation of a monoclonal antibody specific to (1→5)-α-L-arabinan. Carbohydr. Res. 308, 149–152.

Wu, L.G., Joshi, S.P., Chiang, V.L., 2000. A xylem-specific cellulose synthase gene from aspen (*Populus tremuloides*) is responsive to mechanical stress. Plant J. 22, 495–502.